Proceedings of the Institute of Acoustics

Fibre-Optic Sensing for Analysis of Turbulent Pressure Fluctuations in Partially Filled Pipes

Jah Shamas	University of Sheffield, Department of Mechanical Engineering, Sheffield, UK
Anton Krynkin	University of Sheffield, Department of Mechanical Engineering, Sheffield, UK
Gavin Sailor	University of Sheffield, Department of Civil and Structural Engineering, Sheffield, UK
Simon Tait	University of Sheffield, Department of Civil and Structural Engineering, Sheffield, UK
Yan Liu	Southern University of Science and Technology, School of Environment, Shenzen, China
Kirill Horoshenkov	University of Sheffield, Department of Mechanical Engineering, Sheffield, UK

Abstract

The authors present experimental data obtained from the turbulence-induced vibration of a fibre-optic sensor structure flush-mounting the interior of a partially-filled pipe rig. Methodology capable of estimating the free stream velocity and spatial correlations of the turbulent pressure fluctuations within the boundary layer is presented. The proposed methodology is validated through application to fibre-optic cable data from multiple flow regimes, as well LES-obtained near-wall pressure fluctuation data for the equivalent flow regimes.

1 Introduction

While the dynamics of pressurised pipelines is well understood, considerably less attention has been given to pipes running partially-filled. Understanding the hydraulic conditions in partially-filled pipes is of great practical importance for many engineering applications, such as leak detection for sewer pipeline networks. Current methods for monitoring these flows utilises spot sensing, where hydrodynamic measurements are collected at discrete locations. These methods provide little information on the interior hydraulic conditions in real time, leaving operators blind to the conditions of their assets, thorough reviews of commonly utilised methods for monitoring pipelines are given in [1, 2, 3] . Energetic turbulent structures in these pipe flows exert wall-normal pressure fluctuations onto the interior pipe wall, inducing a vibratory response of the structure. It is hypothesised that the hydrodynamic conditions of the flow and the pressure within the boundary layer at the wall are related. It is the goal of the current research to unambiguously establish their relation by use of a novel flush-mounted fibre-optic sensor embedded in the wall of a partially-filled pipe. Turbulent pressure fluctuations within the boundary layer induce a dynamic response of the fibre-optic sensor (FOS) structure, consequently resulting in signal fluctuations of the interior fibre-optic cable. These proceedings demonstrate that application of time delay estimation (TDE) method [4] to the FOS data yields accurate estimates of the flow velocity inside the pipe for two flow regimes. It will also be shown that recovered spatial correlation of sensor response matches spatial correlation patterns of the boundary layer pressure at the pipe wall.

2 Experimental Setup

At the ICAIR test facility, the University of Sheffield, two flow regimes have been tested to investigate the response of a FOS axially lining the interior of a 20m long partially-filled pipe setup to turbulence-induced vibration. The containment system housing the fibre-optic cable consists of a streamwise-installed plate-gel system, with the top surface of the plate flush with the pipe wall exposed to the partially-filled flow inside the 0.15m radius 20m pipe, 5m downstream of the inlet tank. An engionic Femto Gratings GmbH SM1250BI(9.8/125)P fibre-optic cable is installed at the plate-gel boundary that operates on the principles of Bragg reflection. The locations of the six FBG elements in the cable are known, from which axial strain of the cable can be recovered.

In this study The FOS data from two flow regimes have been used to observe how changes in

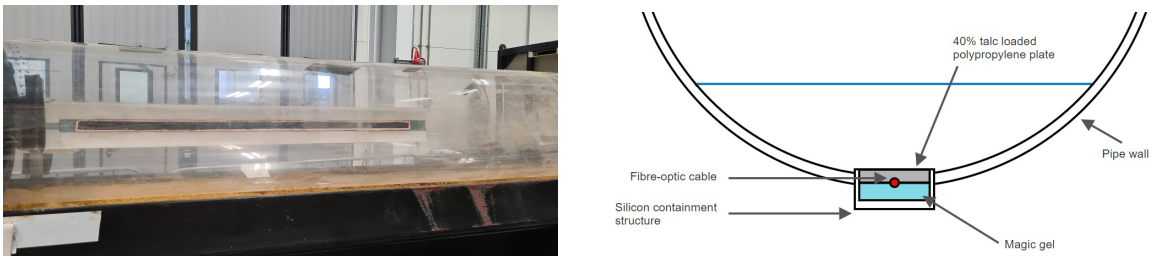

(a) (b)

Figure 1: (a): In-pipe view of the flush-mounted FOS. (b): Schematic cross-sectional view of the sensor structure and pipe.

hydraulic conditions manifest in the cables signal response. The flow regimes are given in Table 1:

Table 1: Flow regimes used during data collection.

Regime	Slope	Depth (m)	Flow Rate (L/s)	Velocity (m/s)	Re (-)
1	0.005	0.15	24	0.68	2×10^5
2	0.005	0.075	7	0.51	1.5×10^5

For both flow regimes, pressure fluctuations at the pipe wall induce signal fluctuations in the cable which were recorded through a Luna si155 ST optical sensing interrogator at a sampling rate of 1kHz. Data were collected from two hours of fully developed flow, followed by a subsequent two hours of fully developed flow with a honeycomb mesh at the inlet tank to decrease free stream turbulence. This was followed by a detrending and filtering process to remove external noise before the signal response was analysed. Additional data have been collected for each flow regime by rotating the pipe section containing the FOS at increments of 8 degrees to span up to the water surface, and repeating the four hour data collection process as outlined above. This extensive collection of experimental data was carried out to provide the authors with the means to understand the angular change in the wall-pressure fluctuations at the pipe wall.

3 Large-Eddy Simulation Data

In addition to experimental data, Large-Eddy Simulation (LES) data of wall-normal pressure fluctuation time series in a partially-filled fully developed pipe flow have been produced by the authors (radius 0.15m) [5] . The hydraulic parameters of the flow used in these simulations are given in Table 2:

Table 2: Flow regime used in Large-Eddy Simulation.

Regime	Slope	Depth (m)	Flow Rate (L/s)	Velocity (m/s)	Re (-)
1	0.00182	0.135	21.2	0.667	2×10^5

Pressure time series data are recovered on a mesh of 80 x 25 grid points in the x and θ directions along the pipe wall. For reference, x denotes streamwise coordinate, and θ denotes the angular coordinate, being the rotation in degrees about the pipe wall from the pipe bottom. The LES-data span a length of 1.58m in the streamwise direction, with a mesh spacing of $\Delta x = 0.02m$. The angular mesh separation in the θ direction is $\Delta\theta = 7^o$ between -84^o and $+84^o$ (pipe bottom at 0^o). Pressure time series were written out at a frequency of 208Hz for a duration of 40s. It should be noted that periodic boundary conditions were also implemented between the extremities of the

streamwise domain ($x_0 = 0m$ and $x_{80} = 1.58m$). For this reason, analysis of LES data was only performed over half of the streamwise domain to negate any effects the periodic boundary conditions may have when analysing streamwise features present in the pressure data.

In the following sections we shall introduce the methodology that has been used to manipulate the raw FOS data to recover an estimate of flow velocity and spatial correlation structure within the partially-filled pipe setup at ICAIR. When presenting findings from experimental data, equivalent findings from applying the same manipulation of LES data will also be presented to showcase the similarities between FOS response to turbulent excitation, and the LES-obtained turbulent pressure fluctuations. It will become evident that even though the experimental FOS data are not a direct measurement of the turbulent pressure itself, the comparison of this with numerical pressure fluctuation data lends itself to the conclusion that the FOS is capable of recovering properties of the turbulence.

4 Flow Velocity Estimation

.

For a given flow condition and angular position of the FOS, data from each of the six FBGs within the fibre were collected at a sampling rate of $f =$ 1kHz for two hours of fully developed flow. Linear trends in these time series were removed, and then fed through a third order Butterworth bandpass filter to filter out low and high frequency noise, resulting in a vector of strains $[x_i(t)]$ for the i'th FBG. As the flow was fully developed during these two hour windows, and homogeneous turbulence is assumed, it is understood the statistics of the turbulence remain constant [6], as do the statistics of the FOS response. It is also understood that patterns common among all gratings would emerge in data of much shorter time scales than 2 hours. To allow for time averaging over shorter segments of the FOS response data, data recorded from the FOS were partitioned into sections of M minutes in length, (M was typically not chosen to be less than 2). The analysis procedure used to recover flow velocity from these data is as follows: Splitting $[x_i(t)]$ up into sections of M minutes allows it to be rewritten in the following matrix form,

$$\hat{x}_i(t)] \;=\; [\,[x_{i,1}]\;[x_{i,2}]\,...\,[x_{i,m}]\,]. \tag{1}$$

Where $m = 120/M$, and each column $[x_{i,k}]$ corresponds to the k'th section of the time series of FBG i, each column consisting of fM time steps.

Utilising the built-in 'xcorr' function in MATLAB, the time lag τ^* maximising the cross-correlation between the k'th section of sensors i and j, $R_{i,j,k}$ was computed as:

$$\tau^* \;=\; \underset{\tau\,\in\,[0,M]}{\operatorname{argmax}}\left(R_{i,j,k}(\tau)\right). \tag{2}$$

Where

$$R_{i,j,k}(\tau) = \left(\frac{1}{M}\int_0^M [x_{i,k}(t)][x_{j,k}(t+\tau)]dt\right). \tag{3}$$

Finding the lag τ^* gives a time delay estimation (TDE) between the time series of the two gratings. Dividing the distance between these two FBGs $d(i,j)$ by this value results in an estimate of the velocity of the propagating turbulent pressure fluctuations at the pipe wall. We can compute this for all combinations of pairs (i,j), $1 \leq i < j \;\leq 6$, then divide $d(i,j)$ by this value to provide an estimate of the flow velocity recorded between all combinations of grating pairs, for all M minute time sections. Cutting the two hour signal up in this fashion allows for more estimates of the flow velocity to be recovered from the raw data. Below are histograms of velocity estimations obtained from applying this methodology to fibre data collected at the pipe bottom for both flow regimes. A 5Hz bandpass window from 3-8Hz was used, split into 60 $M = 2$ minute sections, resulting in 900 estimates of flow velocity displayed in each subfigure below.

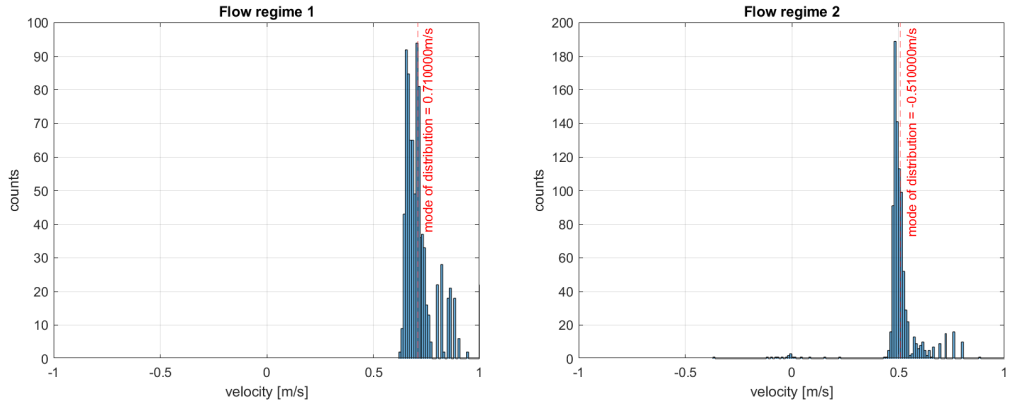

Figure 2: Distribution of flow velocity estimates obtained through manipulating cross-correlation between grating readings from the pipe bottom in (a): flow regime 1, (b): flow regime 2.

The distributions in Figure 2 have a significant mass concentrated around a particular estimate of velocity, having modes at 0.71 and 0.51 m/s, respectively. These are reasonable estimates of the flow velocity in both flow regimes recovered from a TDE of the sensor readings in the plate. It should be highlighted that while the mode estimate for flow velocity was not influenced by the bandpass window used, it is understood that for a centre frequency f_c of the bandpass window outside a certain range, the TDE method produces velocity estimates concentrating around $0\,m/s$ for both regimes. It is hypothesised by the authors that all information pertaining to flow is contained within a certain frequency band, and any information outside of this range corresponds to either electrical noise, or turbulent-induced vibration of the pipe structure itself. Performing the TDE method on these inappropriately filtered time series would result in poor velocity distributions as the features travelling with the flow velocity have been filtered out. This phenomenon is displayed through application of bandpass windows with increasing central frequencies of $f_c = 5.5,\ 6.5,\ 7.5,\ 8.5,\ 9.5\,, 10.5$ Hz.

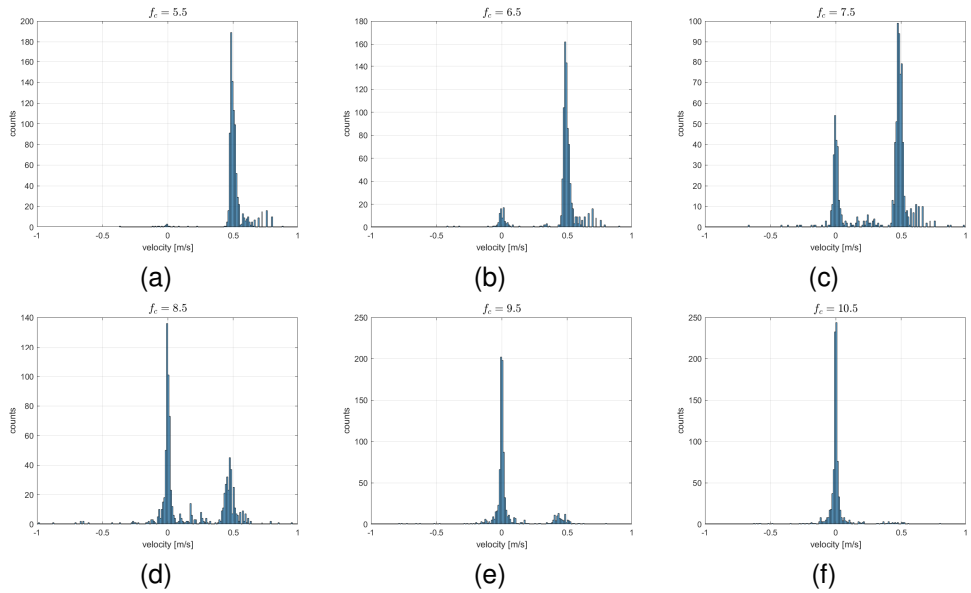

Figure 3: Distribution of flow velocity estimates obtained from increasing the central frequency of bandpass window to grating readings from the pipe bottom in flow regime 2.

It is understood that past a certain bandpass limit (for a given flow regime and angular FOS position), it is impossible to recover any flow information via the TDE method. While the noise present at $0\,m/s$

for incorrect time series filtering reduces the amount of flow information present in the data, it tells us which specific bandpass window retains flow information and expels electrical/structural noise to the greatest extent. Through testing different filter types for each flow regime and angular position of the FOS, the bandpass limits reducing mass in the velocity distribution at $0\,m/s$ can be recovered.

To validate the distributions shown in this section, the above analysis was performed on the numerical pressure fluctuation time series data obtained from LES simulations to obtain analogous velocity distributions as shown in Figure 4. Even though the LES data were recorded over a much shorter time interval than the experimental data, there was a much greater spatial resolution in the LES domain compared to the experimental setup. Thus, a high amount of velocity estimates could be produced due to the greater spatial resolution, even with a much shorter signal.

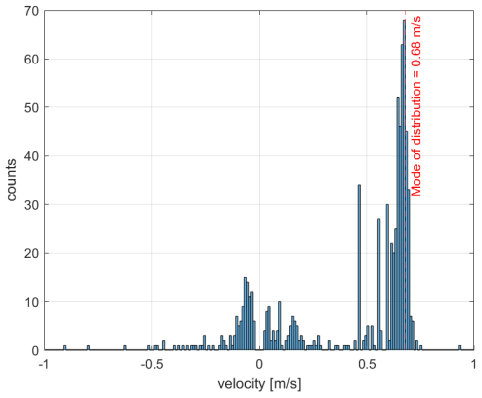

(a)

Figure 4: Distribution of flow velocity estimates obtained through manipulating cross-correlation between LES pressure fluctuation readings from the pipe bottom.

It is believed that the mass concentrated around 0m/s is due to numerical errors resulting from insufficient convergence times of the simulation. Similarly to the distributions in Figure 2, there is a large mass concentrated around the flow velocity of the simulation, 0.68m/s, demonstrating the analysis technique given in this section is capable of recovering an accurate estimate of the flow velocity, given that the time series data are preprocessed appropriately.

5 Spatial Correlations of Turbulent Pressure

In the previous section, the importance of filtering the FOS data in a correct frequency range was highlighted. As detailed in Figure 3, there appears to be an optimal filter range that is capable of recovering flow characteristics from the sensor response, and straying from this range recovers more stationary behaviour of the pipe structure rather than the turbulent features that convect along the surface of the sensor with the flow velocity. Due to an existence of this 'ideal' range for a particular angular position of the FOS, it was decided to analyse the spatial correlation of the time series data filtered in this specific range only. It has been suggested that correlation lengthscales of near-wall pressure fluctuations relate to the size of turbulent structures in the flow, and so it was the aim to determine if patterns of correlation obtained from the sensor match realistic expectations of spatial pressure correlations at the pipe wall.

Due to the assumption of homogeneous turbulence, it is realised that correlation between two points in space only depends on their separation, and not their absolute position in space [7]. Thus, the streamwise array of $n_r = 6$ individual gratings can be utilised to calculate the spatial correlation at $n_p = n_r(n_r - 1)/2 = 15$ distinct non-negative separations in the streamwise direction. Two different computations of the spatial correlation were recovered, first: the time series signal for each non-negative separation pair of gratings (i, j) were cross-correlated, and the maximum value of this

normalised cross-correlation

$$r_{ij} = \max\left(\frac{1}{T}\int_0^T [x_i(t)]\,[x_j(t+\tau)]dt\right) \tag{4}$$

was recovered. This corresponds highest degree of correlation between two locations $d(i,j)$ apart, regardless of time lag between the two signals. By not restricting the lag at which to recover this value of r_{ij}, this form of spatial correlation provides information on how the near-wall pressure fluctuations correlate at different separations as the fluctuations convect with the flow. The second computation recovers the cross correlation value between two gratings' time series at a fixed lag,

$$s_{ij} = R_{ij}(\tau_0) = \frac{1}{T}\int_0^T [x_i(t)]\,[x_j(t+\tau_0)]dt. \tag{5}$$

By constraining the lag at which to recover the value of the cross-correlation for all non-negative grating pairs, it can be understood how pressure fluctuations at the pipe wall correlate over the entire length of the sensor at a given instance in time. In order to more formally characterise the behaviour of maximum spatial correlation r_{ij} for a given angular position, an analytical expression r was proposed as

$$r(x) = e^{-x/L}. \tag{6}$$

In this expression, x is the streamwise separation along the length of the sensor, and the additional parameter L is defined as the correlation length. It has been proposed that the spatial correlation of boundary layer pressure fluctuations takes the form given above [8, 9]. Profiles of $r_{ij}, r, s_{ij}(\tau_0 = 0)$ computed over M = 2 minute intervals are displayed from the pipe bottom of flow regimes 1 and 2.

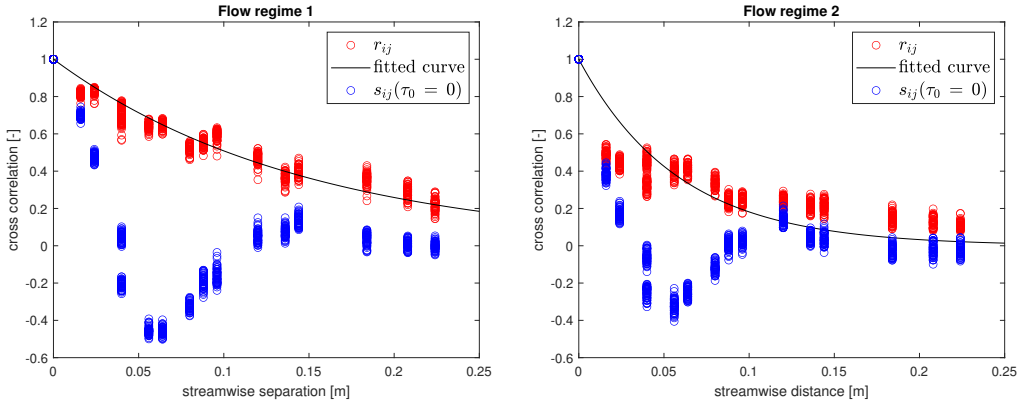

(a) (b)

Figure 5: Spatial correlation estimates and fitting from the pipe bottom in (a): flow regime 1, (b): flow regime 2.

It can be seen in Figure 5 that the correlation diminishes over a shorter length in flow regime 2. This is because the depth limits the size of the largest turbulent eddies in the flow, and these eddies are responsible for the pressure fluctuations that are observed at the pipe wall. The correlation lengths were resolved as $0.148m$ and $0.067m$ for regimes 1 and 2, respectively, providing rough estimates of the flow depth in each case. To validate the streamwise correlation patterns recovered from each flow regime, both forms of correlation r_{ij}, s_{ij} were recovered over the same streamwise range from LES data shown in Figure 6.

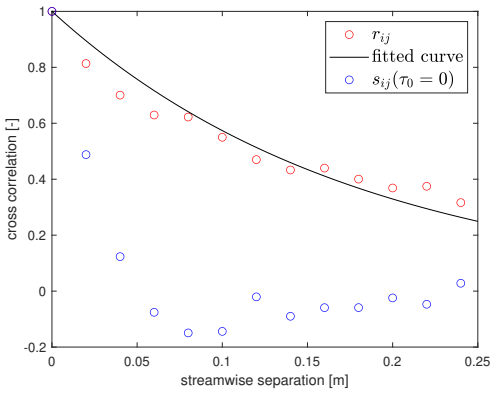

(a)

Figure 6: Spatial correlation estimates and fitting from the pipe bottom of LES data.

It can be seen that the form of r_{ij} obtained in Figure 6 matches well to the form of r_{ij} in Figure 5(a) due to the similarity of the flow conditions. Indeed, the correlation length for the streamwise correlation in this case was recovered as $L = 0.18m$, which is in close agreement with the value of L recovered from flow regime 1.

6 Conclusion and future work

It has been demonstrated that the novel fibre-optic sensor structure installed on the interior of a partially-filled pipe rig responds well to turbulent excitation at the pipe wall. Estimation of key hydraulic parameters from multiple flow regimes has also been recovered through application of signal processing techniques to the sensor data and relating the recovered quantities to flow characteristics.

Work is in progress to compute the frequency-wavenumber spectrum from the array of FBG elements within the fibre-optic cable. This is recovered by computing the 2D Fourier Transform of the spacetime correlation function obtained from the FOS data. Filtering and signal processing techniques are being applied to these recovered spectra to identify convective ridges that correspond to properties of flow velocity contained within the FOS response.

References

[1] Zheng Liu and Yehuda Kleiner. State of the art review of inspection technologies for condition assessment of water pipes. *Measurement: Journal of the International Measurement Confederation*, 46(1):1–15, 2013. ISSN 02632241. doi: 10.1016/J.MEASUREMENT.2012.05.032. URL http://dx.doi.org/10.1016/j.measurement.2012.05.032.

[2] Piervincenzo Rizzo. Water and Wastewater Pipe Nondestructive Evaluation and Health Monitoring: A Review. *Advances in Civil Engineering*, 2010:1–13, 2010. ISSN 1687-8086. doi: 10.1155/2010/818597. URL http://www.hindawi.com/journals/ace/2010/818597/.

[3] Olga Duran, Kaspar Althoefer, and Lakmal D. Seneviratne. State of the art in sensor technologies for sewer inspection. *IEEE Sensors Journal*, 2(2):73–81, 2002. ISSN 1530437X. doi: 10.1109/JSEN.2002.1000245.

[4] G Clifford Carter. Coherence and time delay estimation. *Proceedings of the IEEE*, 75(2): 236–255, 1987.

[5] Yan Liu, T. Stoesser, and H. Fang. Effect of secondary currents on the flow and turbulence in partially filled pipes. *Journal of Fluid Mechanics*, 938:A16, 2022. doi: 10.1017/jfm.2022.141.

[6] George Keith Batchelor. *The theory of homogeneous turbulence*. Cambridge university press, 1953.

[7] Edouard Salze, Christophe Bailly, Olivier Marsden, and Daniel Juvé. INVESTIGATION OF THE WALL PRESSURE WAVENUMBER-FREQUENCY SPECTRUM BENEATH A TURBULENT BOUNDARY LAYER WITH PRESSURE GRADIENT. In *International Symposium On Turbulence and Shear Flow Phenomena (TSFP-9)*, Melbourne, Australia, June 2015. URL https://hal.science/hal-02409442.

[8] Lawrence J. DeChant and Justin A. Smith. Consistent Turbulent Boundary Layer Wall Pressure Spectra and Coherence Functions. In *2018 AIAA Aerospace Sciences Meeting*, pages 1–15, Reston, Virginia, jan 2018. American Institute of Aeronautics and Astronautics. ISBN 978-1-62410-524-1. doi: 10.2514/6.2018-1826. URL https://arc.aiaa.org/doi/10.2514/6.2018-1826.

[9] JM Clinch. Measurements of the wall pressure field at the surface of a smooth-walled pipe containing turbulent water flow. *Journal of sound and vibration*, 9(3):398–419, 1969.